



The protein phosphatase gene *MaPpt1* acts as a programmer of microcycle conidiation and a negative regulator of UV-B tolerance in *Metarhizium acridum*

Jie Zhang^{1,2,3} · Zhenglong Wang^{1,2,3} · Nemat O. Keyhani^{1,4} · Guoxiong Peng^{1,2,3} · Kai Jin^{1,2,3} · Yuxian Xia^{1,2,3} 

Received: 26 September 2018 / Revised: 4 December 2018 / Accepted: 7 December 2018 / Published online: 4 January 2019
© Springer-Verlag GmbH Germany, part of Springer Nature 2019

Abstract

The Ser/Thr protein phosphatase Ppt1 (yeast)/PP5 (humans) has been implicated in signal transduction-mediated growth and differentiation, DNA damage/repair, cell cycle progression, and heat shock responses. Little, however, is known concerning the functions of Ppt1/PP5 in filamentous fungi. In this study, the Ppt1 gene *MaPpt1* was characterized in the insect pathogenic fungus, *Metarhizium acridum*. The MaPpt1 protein features a three-tandem tetratricopeptide repeat (TPR) domain and a peptidyl-prolyl cis-trans isomerase-like (PP2Ac) domain. Subcellular localization using an MaPpt1::eGFP fusion protein revealed that MaPpt1 was localized in the cytoplasm of spores, but gathered at the septa in growing hyphae. Targeted gene inactivation of *MaPpt1* in *M. acridum* resulted in unexpected reprogramming of normal aerial conidiation to microcycle conidiation. Although overall vegetative growth was unaffected, a significant increase in conidial yield was noted in Δ *MaPpt1*. Stress-responsive phenotypes and virulence were largely unaffected in Δ *MaPpt1*. Exceptionally, Δ *MaPpt1* displayed increased UV tolerance compared to wild type. Digital gene expression data revealed that *MaPpt1* mediates transcription of sets of genes involved in conidiation, polarized growth, cell cycle, cell proliferation, DNA replication and repair, and some important signaling pathways. These data indicate a unique role for Ppt1 in filamentous fungal development and differentiation.

Keywords Protein phosphatase Ppt1 · *Metarhizium acridum* · Microcycle conidiation · UV tolerance

Electronic supplementary material The online version of this article (<https://doi.org/10.1007/s00253-018-9567-3>) contains supplementary material, which is available to authorized users.

✉ Kai Jin
jinkai@cqu.edu.cn

✉ Yuxian Xia
yuxianxia@cqu.edu.cn

- ¹ Genetic Engineering Research Center, School of Life Sciences, Chongqing University, Chongqing 401331, People's Republic of China
- ² Chongqing Engineering Research Center for Fungal Insecticide, Chongqing 401331, People's Republic of China
- ³ Key Laboratory of Gene Function and Regulation Technologies under Chongqing Municipal Education Commission, Chongqing 401331, People's Republic of China
- ⁴ Department of Microbiology and Cell Science, University of Florida, Gainesville, FL 32611, USA

Introduction

The competing states of phosphorylation/dephosphorylation of serine and threonine residues in a wide range of proteins mediate diverse and sometimes essential cellular processes and rely upon the activities of protein kinases and phosphatases. In eukaryotes, the phosphoprotein phosphatases (PPP) family members are evolutionarily highly conserved proteins and fall into several subfamilies, including PP1, PP2A, PP2B, PP4, PP5, PP6, and PP7 (Barford 1996; Kennelly 2001). Among those, the PP5 (Ppt1 in yeast) subfamily contains as a single member throughout the *Eukaryota* (de la Fuente van Bentem et al. 2003; Shi 2009) and structurally features two domains not found in other PPP family: one is a peptidyl-prolyl cis-trans isomerase-like (PP2Ac) domain and another is a three-tandem tetratricopeptide repeat (TPR) domain which acts as a protein-protein interaction motif at the N-terminus (Das et al. 1998). PP5 first characterized in mammalian

systems has been shown to be expressed in virtually all mammalian tissues, with high levels seen in the brain (Becker et al. 1994). Ascribed functions of PP5 include affected cellular responses to DNA damage, heat shock, and osmotic balance, participating in processes as diverse as cell proliferation and migration, and apoptosis and survival (Ali et al. 2004; Chinkers 2001; Kang et al. 2011; Wandinger et al. 2006).

Less is known about the yeast/fungal PP5/Ppt1 homolog. In *Neurospora crassa*, expression of Ppt1 is induced in conidia but suppressed during conidial germination (Dickman and Yarden 1999). Targeted gene inactivation of Ppt1 in *Saccharomyces cerevisiae* resulted in only limited phenotypes under various stress conditions, indicating its non-essential role (Jeong et al. 2003). The yeast Ppt1 has been shown to regulate heat shock protein 90 (HSP90), an important molecular chaperone, and other PPP enzymes (Wandinger et al. 2006), to localize in both the nuclei and cytoplasm and exhibit an activity similar to that of human PP5 despite C-terminal functioning differences between Ppt1 and PP5 (Chen et al. 1994; Jeong et al. 2003). In contrast, however, the three-tandem TPR domain of the Ppt1 homolog in *Aspergillus oryzae* showed no auto-inhibitory activity, since its activity was not enhanced by adding lipids (Feng et al. 2007). In *Candida albicans*, deletion of the *CaPpt1* exerted little influence on hyphal formation, cell responses to the genotoxins, methylmethane sulfonate, and hydroxyurea, or the activation of DNA damage response pathways, but resulted in increased sensitivity to UV irradiation, calcofluor white, and salt stresses (Hu et al. 2014). These results suggest that the functions of the Ppt1 homologs are highly diverged in fungi.

Insect pathogenic fungi are important biological control agents of insect pests (Lomer et al. 2001; Li et al. 2010). Asexually produced fungal conidia are generally responsible for initiating infection on the cuticle of a suitable host, where conidia attach and germinate for hyphal expansion to activate the pathways that ultimately allows the pathogen to penetrate the host exoskeleton (Ortiz-Urquiza and Keyhani 2013). Stress responses have been shown to be critical for successful use of these fungi, and approaches to enhance resistance and/or increase virulence have met with some success (Ortiz-Urquiza et al. 2015; Rangel et al. 2015; Zhang and Feng 2018). To date, little is known about the roles of Ser/Thr protein phosphatases in insect pathogenic fungi. The insect pathogenic fungus *Metarhizium acridum* is an acridid-specific pathogen that can produce several types of spore structures depending upon the environmental conditions (Zhang et al. 2010). Aerial conidia represent the most common form of spores and are produced in most standard mycological media as well as on host cadavers. Microcycle conidia are produced only under unfavorable environmental conditions (Bosch

and Yantorno 1999). In this study, *MaPpt1*, a single-copy PPase gene, was found to act as a regulator of asexual development and/or cell differentiation. The absence of *MaPpt1* resulted in reprogramming of normal aerial conidiation to microcycle conidiation and hence a marked increase in conidial yield with little influence on vegetative growth. Stress-responsive phenotypes and virulence were largely unaffected in $\Delta MaPpt1$, which became more resistant to UV irradiation than its wild-type parent. Digital gene expression profiling revealed alteration in a network of genes involved in conidiation, polarized growth, cell cycle, cell proliferation, DNA replication and repair, and some important signaling pathways. Our data indicate an important role for Ppt1 in the developmental and cellular processes of the locust mycopathogen.

Materials and methods

Strains and cultivation

M. acridum CQMa102 (China General Microbiological Culture Collection Center, CGMCC, No. 0877) was used as the wild type (WT). Fungal strains were typically grown in Czapek-Dox agar medium (CZA) and one-quarter-strength Sabouraud's dextrose agar medium (1/4 SDAY consisting of 1% dextrose, 0.25% mycological peptone, 0.5% yeast extract, and 2% agar, w/v). Bacterial strains, *Escherichia coli* JM109 (TransGen Biotech, Beijing, China) and *Agrobacterium tumefaciens* AGL-1 (Lazo et al. 1991), were used for routine cloning, plasmid propagation, and fungal transformation.

Bioinformatic analysis

Amino acid sequences of fungal Ppt1 homologs were retrieved from the NCBI database as follows: *M. acridum* (XP_007806792), *Metarhizium robertsii* (XP_007823541), *Ustilagoideia virens* (KDB16796), *Fusarium oxysporum* (EMT65044), *Beauveria bassiana* (XP_008600484), *Cordyceps militaris* (XP_006669089), *Trichoderma harzianum* (KKO99205), *Verticillium alfalfa* (XP_003008390), *Pseudogymnoascus destructans* (ELR10400), and *Blumeria graminis* (CCU77363). Sequences were analyzed using NCBI/DNAMAN V6 software for motif scanning and amino acid multiple alignments, followed by phylogenetic analysis with the maximum likelihood method in MEGA7 software at <http://www.megasoftware.net/>. Functional domains of MaPpt1 were analyzed using SMART (<http://smart.embl-heidelberg.de/>). Protein structure predictions were generated using the SWISS-MODEL Automatic Modelling Mode (<http://swissmodel.expasy.org>) and evaluated using the QMEAN6 score (Schwede et al. 2003).

Plasmid construction and fungal transformation

To construct the targeted gene disruption vector, the 5' (1 kb) and 3' (0.9 kb) fragments of the *MaPpt1* gene were amplified with primer pairs, LF/LR and RF/RR (Supplementary Table S1). The amplified fragments contained *HindIII/XbaI* and *EcoRV/EcoRI* sites, respectively. PCR reaction was performed using KAPA HiFi HotStart ReadyMix PCR Kit (Kapa Biosystems, Wilmington, MA, USA). PCR products were digested with restriction enzymes as per primer content and cloned into respective sites in plasmid pK2-PB (Ming et al. 2014) harboring the glufosinate ammonium resistance gene (*bar*) to yield pK2-PB-*MaPpt1L/R*. To construct the complementation vector pK2-sur-*MaPpt1::egfp*, a ~4.2-kb fragment including the full-length open reading frame (ORF) (~1.8 kb) and the upstream promoter (~2.4 kb) of *MaPpt1* was amplified from the WT genomic DNA using primer pair FF/FR (Supplementary Table S1). Then, the PCR fragment was cloned into the *HindIII/BamHI*-digested pK2-sur-*egfp* vector (Du et al. 2018) to produce pK2-sur-*MaPpt1::egfp*. The final vectors (pK2-PB-*MaPpt1L/R* and pK2-sur-*MaPpt1::egfp*) were transformed into *A. tumafaciens* AGL-1 for fungal transformation (dos Reis et al. 2004), respectively. The *MaPpt1*-disruption transformants (Δ *MaPpt1*) were screened on CZA containing 500 μ g/ml glufosinate ammonium (Sigma, St. Louis, MO, USA) and detected by PCR using primers L1/PR and BF/R1 (Supplementary Table S1). The complementary transformants (CM) were screened on CZA containing 20 μ g/ml chlorimuron ethyl (Sigma, Bellefonte, PA, USA). *MaPpt1*-disruption and complementary transformants were further confirmed by Southern blotting and quantitative real-time PCR (qRT-PCR) using primers QF/QR (Supplementary Table S1). The *M. acridum* glyceraldehyde-3-phosphate dehydrogenase gene *Magpd* (EFY84384) was used as an internal control and detected using primers Gpd-F/Gpd-R (Supplementary Table S1).

Southern blotting

To perform a Southern blot analysis, 3–5 μ g of digested genomic DNA and a DNA ladder were fractionated on a 1% agarose gel, transferred to a nylon membrane, and hybridization, then performed following the instructions of the Roche DIG High Prime DNA Labeling and Detection Starter Kit I (Roche, Mannheim, Germany). The probe was amplified using the primers Probe-F/Probe-R (Supplementary Table S1).

Subcellular localization of MaPpt1

Subcellular localization of *MaPpt1* was analyzed using a CM strain, which expressed an *MaPpt1::eGFP* fusion protein under the control of the native *MaPpt1* promoter. Expression and

subcellular localization of *MaPpt1::eGFP* fusion proteins in conidia, germ tubes, and mycelia were visualized through fluorescent microscopy (Nikon Eclipse Ci-E, Tokyo, Japan).

Determination of conidial germination and conidial yield

Conidial germination and conidial yield assays were performed as described previously (Liu et al. 2010). In brief, the conidia of WT, Δ *MaPpt1*, and CM were suspended in sterile water and then filtered through four-layer lens cleaning paper. Fifty-microliter aliquots of conidial suspensions (1×10^7 conidia/ml) were spread evenly on 1/4 SDAY plates and incubated at 28 °C. Conidial germination rates were examined every 2.5 h until full germination. Conidial germination was examined and photographed every 2 h under a microscope (Nikon Eclipse Ci-E, Tokyo, Japan). For conidial yield assessment, 50 μ l fresh conidial suspensions (1×10^7 conidia/ml) were spread on 1/4 SDAY plates and cultured at 28 °C. Conidia production on plates was examined every 3 days from days 3 to 15 on 1/4 SDAY plates.

Heat shock and UV-B tolerance assays

Fungal tolerance to heat and ultraviolet irradiation was determined according to Liu et al. (2010). IT_{50} (50% inhibition time in germination) was compared among WT, Δ *MaPpt1*, and CM. In brief, a 100- μ l aliquot of conidial suspension (1×10^7 conidia/ml) in a sterile Eppendorf tube was placed in a water bath at 45 °C for 0, 2, 4, or 6 h. After the heat shock, a 20- μ l aliquot was spread evenly on 1/4 SDAY plates. After 24-h incubation at 28 °C, the conidial germination rates were calculated via microscopic observation. For UV-B tolerance assays, a 20- μ l aliquot of conidial suspension (1×10^7 conidia/ml) was spread evenly onto 1/4 SDAY plates. The plates were immediately exposed to 1350 mW/m² of UV-B irradiation for 0, 3, 6, or 9 h. The plates were incubated at 28 °C for 24 h. The conidial germination rates were calculated via microscopic observation.

UV-B treatment and single cell gel electrophoresis assay

The single cell gel electrophoresis assay was used to monitor the extent of DNA strand breaks after UV-B treatment in Δ *MaPpt1* and WT as described previously (Kang et al. 2011). Briefly, a UV-B lamp (wavelength, 290–320 nm, 8 W) was used as the source of UV-B irradiation at a rate of 5 J/m². A 50- μ l aliquot of conidial suspensions (1×10^7 conidia/ml) was spread on 1/4 SDAY plates, then irradiated with 5 J/m² and at last, harvested at the indicated times after UV irradiation. Following UV-B treatment, the conidia were stained with 4',6-diamidine-20-phenylindole dihydrochloride

(DAPI) and viewed under a fluorescence microscope (Nikon Eclipse Ci-E, Tokyo, Japan). DNA strand breaks were quantified via fluorescent microscopy of the intensity of the “comet” tail relative to the “head” (reflecting damaged DNA). Analysis of the percentage of DNA that was tail DNA in each cell was performed using Image J software (<http://rsb.info.nih.gov/nih-image>).

Insect bioassays

Bioassays were performed as described previously (Ming et al. 2014). Briefly, newly emerged fifth-instar nymphs of *Locusta migratoria manilensis* (Meyen) were used for bioassays by dropping with 3 μ l paraffin oil conidia suspensions (1×10^7 conidia/ml) under their pronotums (control insects were dropped with 3 μ l paraffin oil). Each treatment had three replicates with 30 insects each, and the experiments were repeated three times. Survival was recorded at 12-h intervals.

Digital gene expression profiling

Fifty-microliter aliquots of conidial suspensions (1×10^7 conidia ml⁻¹) from WT or Δ MaPpt1 were spread evenly onto 1/4 SDAY plates and incubated at 28 °C. Fungal cultures were collected at 16 h and 6 days after inoculation and washed with sterile ddH₂O. Total RNA extraction and digital gene expression (DGE) profiling were performed as described previously (Luo et al. 2013). Genes with a false discovery rate (FDR) < 0.001 and fold change > 2 were considered as differentially expressed genes (DEGs) (Audic and Claverie 1997). DEGs were classified and annotated using gene ontology (GO) analysis. The DGE profiling data reported in this paper have been deposited as raw reads in the GenBank database (BioProject accessions: PRJNA394589, PRJNA394590, PRJNA394591, PRJNA394592).

Verification by qRT-PCR

qRT-PCR was performed to verify the results of DGE profiling. The total RNA for qRT-PCR was the same as RNA used for DGE profiling and obtained as described above. The purified RNA samples were reverse-transcribed using the Prime Script RT Reagent Kit with gDNA Eraser (TaKaRa, Dalian, China) following the manufacturer’s protocol. Twenty-two genes including 12 upregulated and 10 downregulated genes from DGE profiling data were selected randomly for the qRT-PCR assay. Gene-specific qRT-PCR primers (18–20 bp) (Supplementary Table S4) were designed using Beacon Designer 7 software (Premier Biosoft International, Palo Alto, CA, USA). qRT-PCR was performed using SYRB Premix Ex TaqTM II (TaKaRa, Dalian, China) in a CFX ConnectTM Real-Time PCR System (Bio-Rad, Hercules, CA, USA). PCR conditions were 2 min at 95 °C, followed

by 40 cycles of heating at 95 °C for 10 s and annealing at 58 °C for 40 s. Three replicates were performed, and the amplicons were used for melting curve analysis to check the amplification specificity. The relative expression level of each gene was calculated as $2^{-(\Delta\Delta C_t)}$ method (Livak and Schmittgen 2001), and the glyceraldehyde-3-phosphate dehydrogenase gene *Magpd* (EFY84384) from *M. acridum* was used to normalize the amount of template cDNA added in each reaction.

Statistical analysis

All statistics were performed using SPSS 18.0 data processing system software (SPSS Inc, Chicago, IL, USA). ANOVA analysis was used to examine significance between various experimental datasets. A *P* value of less than 0.05 was regarded as statistically significant (different small letters or single asterisk), less than 0.01 regarded as markedly significant differences (different capital letters or double asterisks). All graphs were performed by GraphPad Prism version 5.00 for Windows (GraphPad Software, San Diego, CA, USA, www.graphpad.com).

Results

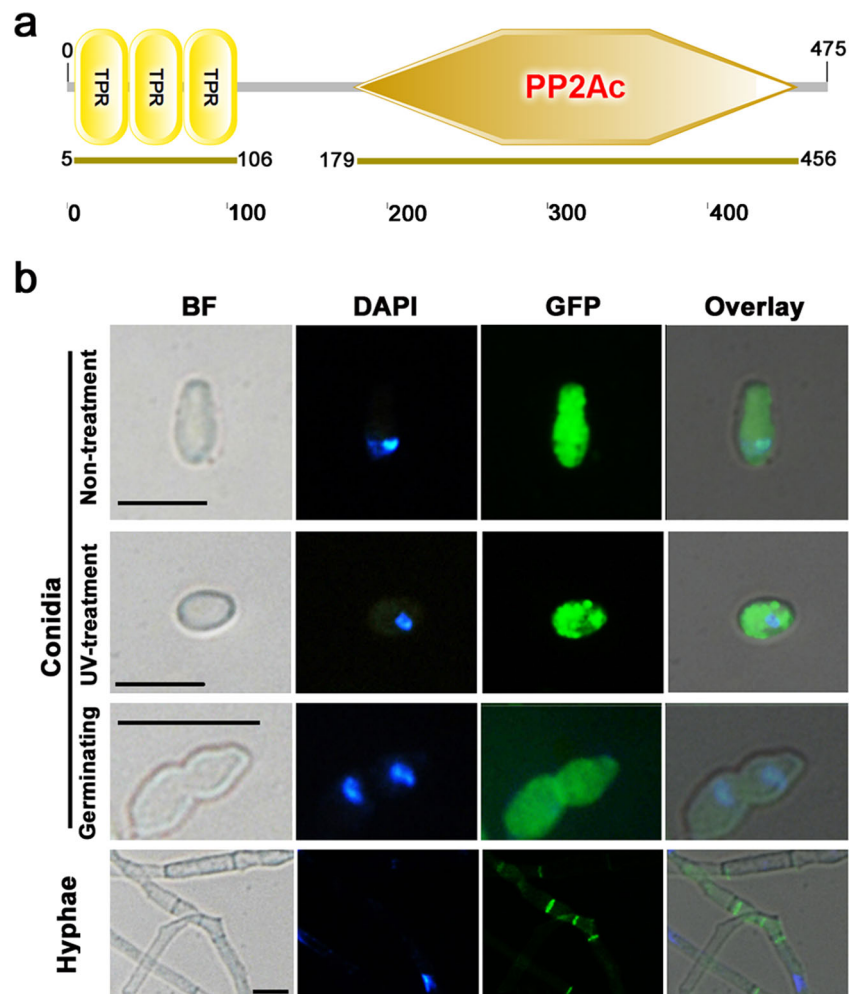
Structural features and subcellular localization of MaPpt1

A single-copy *MaPpt1* gene was found by searching the *M. acridum* genome database (Gao et al. 2011). The MaPpt1 protein contains a three-tandem TPR domain at the N-terminus (residues, 5–106) and a PP2Ac domain at the C-terminus (residues, 179–456) (Fig. 1a). Homology analysis showed that MaPpt1 (XP_007806792) shared 75–98% sequence identities with other fungal Ppt1 proteins (Supplementary Fig. S1a). Phylogenetic analysis revealed that MaPpt1 clustered together with those from *M. robertsii* and *U. virens* (Supplementary Fig. S1b). Quaternary structure prediction showed an 82.5% identity between MaPpt1 and PP5 from rat (accession number, 4JA9_A) using the Swiss Model (Supplementary Fig. S1c). Subcellular localization of MaPpt1 showed that high *MaPpt1::egfp* expression was seen in conidia, where the signal was diffuse throughout the cell during conidial germination and after UV treatment (Fig. 1b). Surprisingly, in growing hyphae, the MaPpt1::eGFP protein localized to septa (Fig. 1b).

Construction of MaPpt1 targeted gene deletion and complementation strains

A targeted gene replacement strategy based on homologous recombination was adopted to generate an *MaPpt1* deletion

Fig. 1 Characteristics of MaPpt1. **a** Schematic structure of MaPpt1. **b** Subcellular localization of MaPpt1 protein in conidia and hyphae of *M. acridum*. A complementary strain carried a C-terminal fusion of MaPpt1 with eGFP protein was used for MaPpt1 localization assay. Conidia and hyphae were stained by DAPI. The overlaid image of eGFP and DAPI staining showed that MaPpt1-eGFP localized in the nucleus. Bar = 10 μ m



mutant, and a corresponding complementary strain was constructed via ectopic insertion of an ~ 4.2 kb fragment including the full-length ORF of the gene (~ 1.8 kb) and upstream promoter (~ 2.4 kb) (Supplementary Fig. S2a). The expected recombinant events were verified by Southern blot and qRT-PCR analyses, indicating that the *MaPpt1* gene was correctly replaced by the *bar* cassette (Supplementary Fig. S2b, c).

Loss of *MaPpt1* results in accelerated germination and increased conidial yield

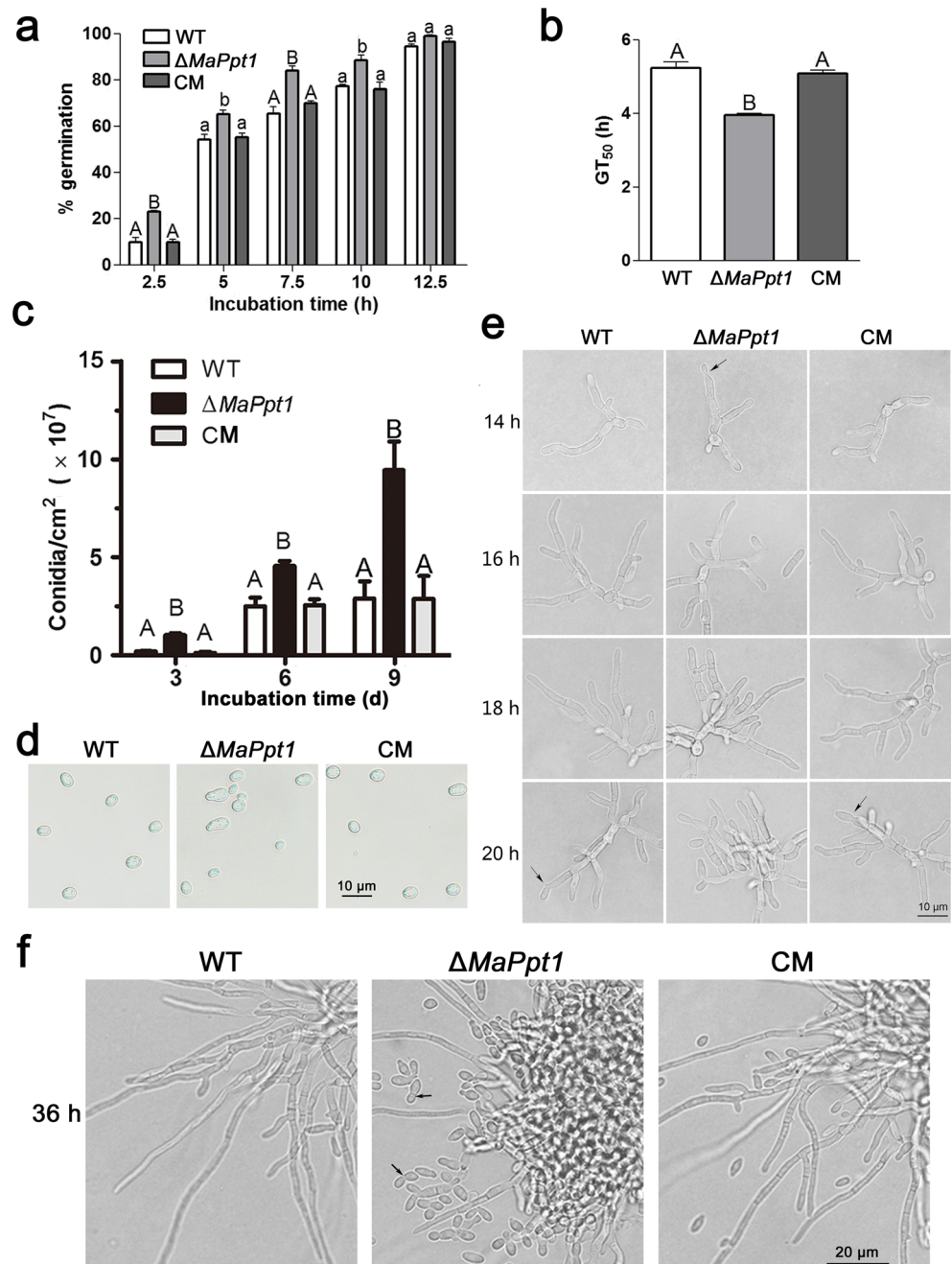
The Δ *MaPpt1* exhibited a significant increase in germination rate of conidia compared to the WT strain (Fig. 2a), and its GT_{50} (time for 50% conidial germination) was about 1 h shorter than for the WT estimate ($P < 0.01$; Fig. 2b). Time-course measurements revealed a significantly increased conidial yield (40–70%) in the Δ *MaPpt1* ($P < 0.001$; Fig. 2c). It was noted that the conidia of Δ *MaPpt1* on 1/4 SDAY were uneven in size compared to those of WT and CM (Fig. 2d; Supplementary Fig. S3). The conidial germination of each

strain on 1/4 SDAY plates was observed during incubation from 14 to 36 h. The germ tubes and hyphal expansion of the Δ *MaPpt1* were morphologically indistinguishable from the WT counterparts until 14 h cultivation at 28 $^{\circ}$ C (Fig. 2e). At 14 h, intriguingly, Δ *MaPpt1* began to form conidia on the hyphal apex (arrow in Fig. 2e) and fell off 2 h later, but a similar phenomenon was observed at 20 h in WT and CM (arrows in Fig. 2e). At 36 h, Δ *MaPpt1* produced many more conidia via microcycle conidiation (arrows in Fig. 2f) than WT and CM via normal conidiation (Fig. 2f).

Loss of *MaPpt1* enhances UV-tolerance but has no effect on thermo-tolerance and virulence

Exposure of conidia to UV-B irradiation revealed a significant increase in UV tolerance of Δ *MaPpt1* as compared to WT and CM over the entire time course examined ($P < 0.01$; Fig. 3a). The IT_{50} was averaged as 5.51 ± 0.13 h and 5.66 ± 0.24 h in WT and CM, respectively, but increased to 7.73 ± 0.36 h in Δ *MaPpt1* ($P < 0.01$; Fig. 3a). However, their germination

Fig. 2 Germination and conidiation. **a** Conidial germination assays of each strain on 1/4 SDAY medium at 28 °C for 2.5, 5, 7.5, 10, and 12.5 h. **b** The time for 50% conidial germination (GT_{50}) from different strains. **c** The conidial yield of different strains on 1/4 SDAY medium at 28 °C for 3, 6, and 9 days. Error bars represent standard deviation. Different capital letters denote significant differences at $P < 0.01$. **d** The conidia of different strains were observed by light microscopy. **e** Mycelial and conidial morphology was observed by light microscopy and photographed at 14, 16, 18, 20, and 22 h. Arrows: conidia on the conidiophores. **f** Mycelial and conidial morphology was observed by light microscopy and photographed at 36 h. Arrows: microcycle conidiation. All strains were inoculated on 1/4 SDAY medium and cultured at 28 °C. WT: wild type; $\Delta MaPpt1$: *MaPpt1*-disruption transformant; CM: complementary transformant



rates were not different in response to heat shock (45 °C) for up to 6 h (Fig. 3b). Insect bioassays revealed no significant change in virulence of $\Delta MaPpt1$ versus WT and CM ($P > 0.05$; Fig. 3c).

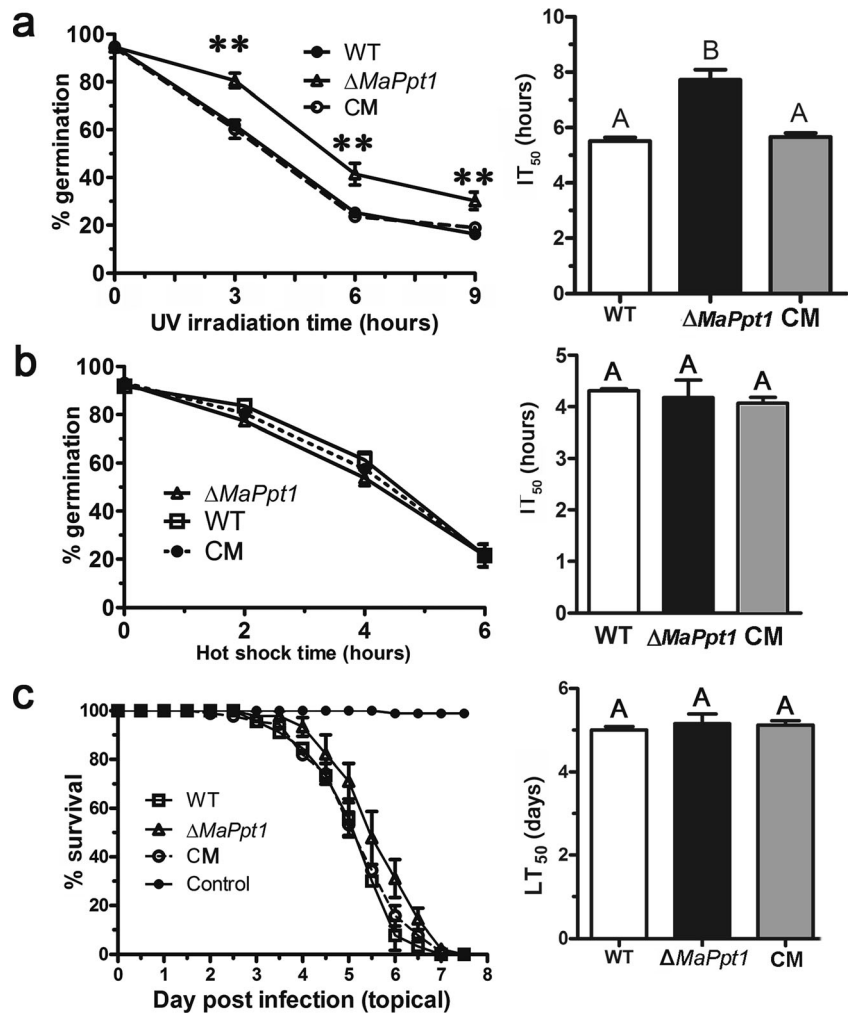
To gain an insight into the increased UV tolerance of the $\Delta MaPpt1$, a single cell gel electrophoresis assay was used to monitor the extent to DNA strand breaks in $\Delta MaPpt1$, WT, and CM. In the absence of UV-irradiation, little tail signal could be detected in all DNA samples (Fig. 4a). After 6-h exposure to UV, a significant increase in DNA strand breaks was noted in $\Delta MaPpt1$ ($75 \pm 4\%$ of tail DNA) as compared to

WT and CM ($62 \pm 4\%$ of tail DNA); however, by 20 h of cultivation, a significant drop in DNA strand breaks was seen in $\Delta MaPpt1$ ($27 \pm 5\%$ of tail DNA), contrasting no change in WT and CM ($63 \pm 3\%$ of tail DNA) ($P < 0.01$; Fig. 4b).

Identification of DEGs influenced by MaPpt1

To understand the mechanism by which MaPpt1 affects fungal conidiation and UV tolerance, the DEGs influenced by MaPpt1 were identified using the DGE method. The transcriptional changes between $\Delta MaPpt1$ and WT at 16 h ($\Delta MaPpt1$ -

Fig. 3 UV irradiation, heat shock, and virulence assays. **a** Conidial germination after UV irradiation at a given time (left panel). The mean 50% inhibition time (IT₅₀) under UV irradiation (right panel). **b** Conidia germination after heat shock at a given time (left panel). The mean 50% inhibition time (IT₅₀) under heat shock (right panel). **c** Insect survival after topical application of conidial suspension from WT, $\Delta MaPpt1$, and CM (left panel). The mean 50% lethality time (LT₅₀) of the WT, $\Delta MaPpt1$, and CM strains after topical inoculation (right panel). For each data point, three biological replicates were assayed. Error bars represent standard deviation. Double asterisks or different capital letters denote significant differences at $P < 0.01$. WT: wild type; $\Delta MaPpt1$: *MaPpt1*-disruption transformant; CM: complementary transformant



16 h vs. WT-16 h) and 6 days ($\Delta MaPpt1$ -6 days vs. WT-6 days) on 1/4 SDAY were analyzed. Overall, DGE analysis mapped transcripts to 1846 of the 9849 *M. acridum* genes.

The comparisons between the various samples revealed that the deletion mutant had 309 genes upregulated and 506 down-regulated at 16 h, and 699 genes upregulated and 522

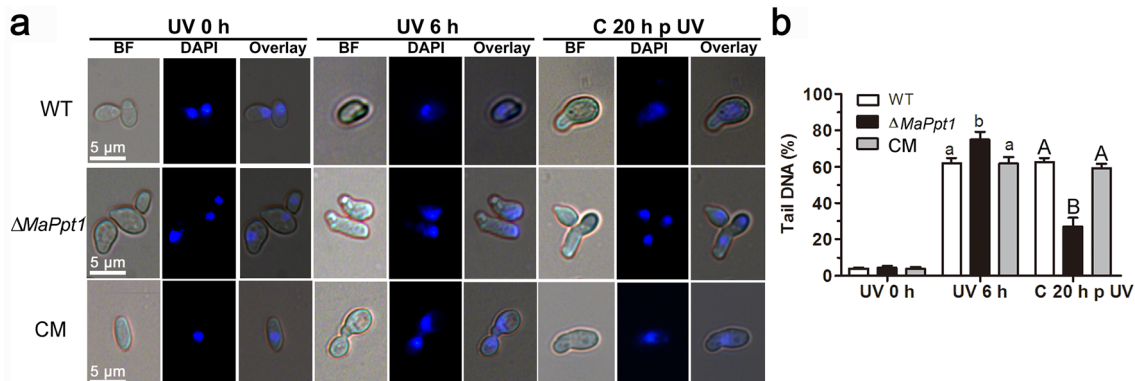


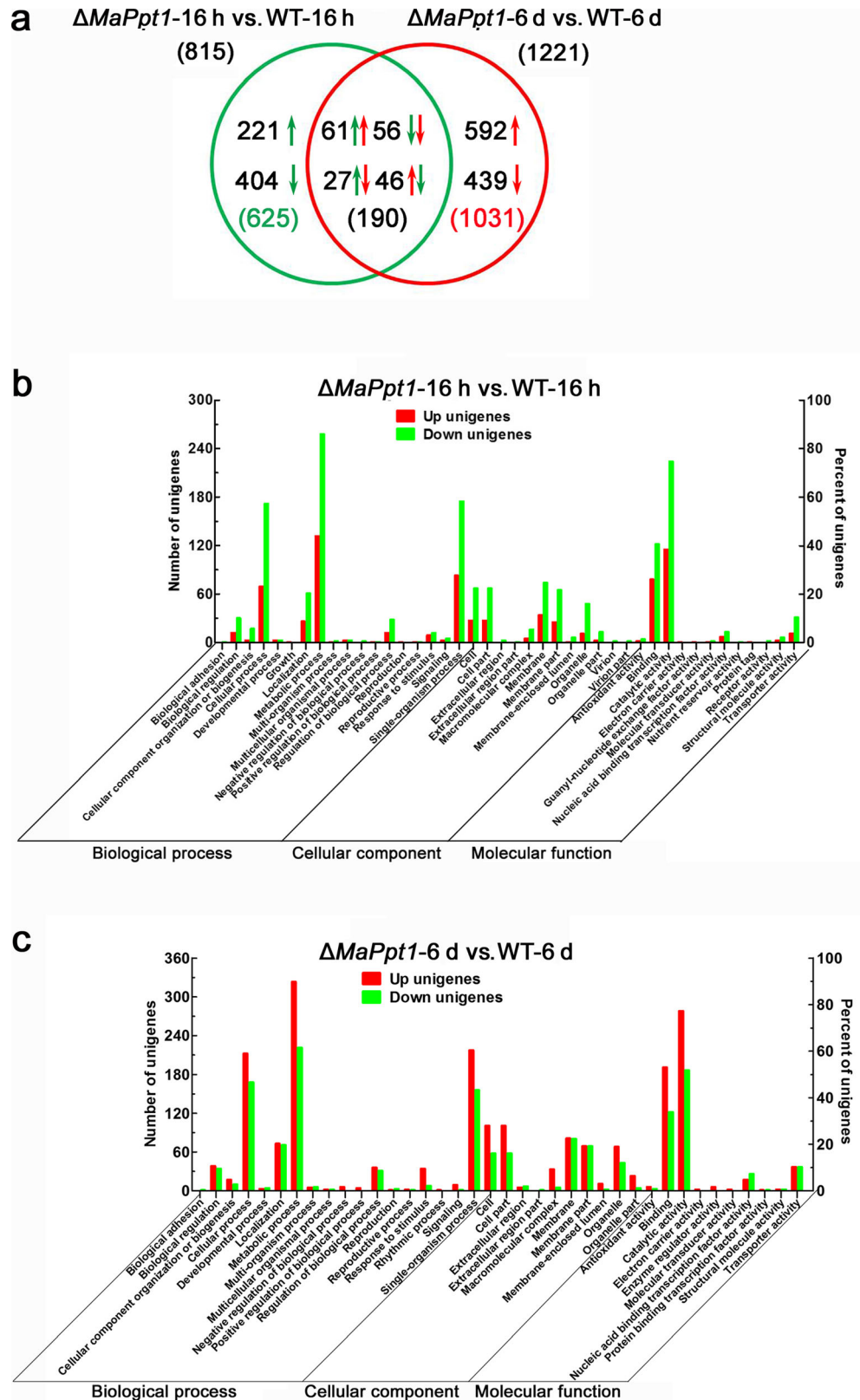
Fig. 4 DNA damage assay under UV irradiation. **a** DNA was stained with DAPI and all images were acquired with fixed exposure times. **b** The quantification of the tail DNA. DNA fragmentation was quantified by determining the tail DNA percentage at least 100 conidia per sample. For each data point, three biological replicates were assayed. “UV 0 h” means the conidia were not treated by UV irradiation. “UV 6 h” means

the conidia were treated by UV irradiation for 6 h and immediately stained using DAPI. “C 20 h p UV” means the conidia were treated by UV irradiation for 6 h, and then cultured in 1/4 SDAY at 28 °C for 20 h. Error bars represent standard deviation. Different capital letters denote significant differences at $P < 0.01$. WT: wild type; $\Delta MaPpt1$: *MaPpt1*-disruption transformant; CM: complementary transformant

downregulated at 6 days (Fig. 5a). Comparative analysis across datasets indicated a total of 190 genes were differentially expressed, including 61 upregulated and 56

downregulated in both datasets ($\Delta MaPpt1$ -16 h vs. WT-16 h and $\Delta MaPpt1$ -6 days vs. WT-6 days), and 27 upregulated genes and 56 downregulated genes in $\Delta MaPpt1$ -16 h vs.

Fig. 5 DGE analysis and GO annotation of DEGs. **a** Venn diagram showing the number of shared DEGs between $\Delta MaPpt1$ -16 h vs. WT-16 h and $\Delta MaPpt1$ -6 days vs. WT-6 days. Shown in the parentheses are the total numbers of differentially expressed genes. *Up arrows* means upregulated genes and *down arrows* indicate downregulated genes in $\Delta MaPpt1$ -16 h vs. WT-16 h (green) or $\Delta MaPpt1$ -6 days vs. WT-6 days (red). **b** GO annotation of the DEGs from $\Delta MaPpt1$ -16 h vs. WT-16 h. **c** GO annotation of the DEGs from $\Delta MaPpt1$ -6 days vs. WT-6 days



WT-16 h dataset, while exhibited opposite pattern in $\Delta MaPpt1$ -6 days vs. WT-6 days dataset (Fig. 5a). The details of DEGs are given in Supplementary Tables S2 and S3. In order to confirm the results from DGE profiling, twenty-two DEGs were selected for qRT-PCR analysis. All the genes showed similar expression patterns in both analyses (Supplementary Table S4), indicating that the data from DGE profiling was reproducible and reliable. GO annotation showed that the DEGs from $\Delta MaPpt1$ -16 h vs. WT-16 h dataset were divided into 42 categories with 18 in biological process, 12 in molecular function, and 12 in cellular component (Fig. 5b), and that the DEGs from $\Delta MaPpt1$ -6 days vs. WT-6 days dataset were assigned to 38 categories with 18 in biological process, 10 in molecular function, and 10 in cellular component (Fig. 5c). Fifteen DEGs involved in arginine, ornithine, linolenic acid, and vitamin B6 metabolism and regulation of autophagy were found only in the $\Delta MaPpt1$ -16 h vs. WT-16 h dataset. For the $\Delta MaPpt1$ -6 days vs. WT-6 days dataset, 48 DEGs involved in DNA replication and repair, sesquiterpenoid/triterpenoid, and *O*-glycan biosynthesis, as well as taurine and arachidonic acid metabolism were identified.

From DGE data, some genes involved in conidiation, polarized growth, cell cycle, and cell proliferation were strongly affected by MaPpt1 (Supplementary Table S5). Of these DEGs, eight genes related to normal aerial conidiation were significantly downregulated in the $\Delta MaPpt1$ strain, such as Grg1 proteins (MAC_06584, MAC_03524, MAC_00515), conidiation-specific protein 10 (MAC_08011, MAC_03245), C6 transcription factor (MAC_05634), bHLH family transcription factor (MAC_06537), and nitrate assimilation regulatory protein nirA (MAC_07722). Multiple genes for cell cycle and cell proliferation, such as the LTE1 protein (MAC_03601), the cell division control protein Cdc48 (MAC_02555), the frequency clock protein (MAC_01916), and three DNA replication licensing factors (MAC_01210, MAC_05980, MAC_01075), were upregulated in the $\Delta MaPpt1$ strain. *FluG* (MAC_08691), a gene involved in inhibition of vegetative growth, and a G protein signaling protein RgsD (MAC_02293) were strongly activated by deletion of *MaPpt1* (Supplementary Table S5). The gene encoding a sulfatase (MAC_04124), implicated in the storage of biologically active steroid hormones and involved in the maintenance of cell adherence junctures, was downregulated. These aforementioned DEGs potentially contributed to the enhanced formation of microcycle conidia in the $\Delta MaPpt1$ strain.

In addition, genes involved in DNA damage repair were also strongly affected by MaPpt1. Of note, 21 DNA damage repair-related genes, such as for recombinational repair protein (MAC_00137), DNA repair protein Rad7 (MAC_06025), DNA repair protein Nse1 (MAC_07762), ATP-dependent DNA ligase domain protein (MAC_05961), and DNA repair

protein UVS6 (MAC_09543), were upregulated in $\Delta MaPpt1$ (Supplementary Table S6), in agreement with the observed greater UV tolerance of the $\Delta MaPpt1$ mutant. In addition, several genes involved in cell wall modification, such as a covalently linked cell wall protein (MAC_03347) and oxdC (MAC_05481), were also altered in expression.

Discussion

To date, a few studies have been reported on the functions of Ppt1 in fungi. Loss of Ppt1 in *S. cerevisiae* showed limited consequences (Jeong et al. 2003), although the targeting of Hsp90 by ScPpt1 has been confirmed (Wandinger et al. 2006). In *C. albicans*, deletion of the *CaPpt1* increased fungal sensitivity to UV irradiation, calcofluor white, and salt stresses (Hu et al. 2014). In this study, the function of the protein phosphatase MaPpt1 was investigated in *M. acridum*. Our results showed that disruption of *MaPpt1* resulted in increasing conidial yield due to reprogramming of normal aerial conidiation to microcycle conidiation and being more resistant to UV irradiation than its wild-type parent.

Deletion of *MaPpt1* increased conidial yield owing to enhancing microcycle conidiation. DGE results showed that the deletion of *MaPpt1* resulted in major changes in transcriptional level of *M. acridum*, reflecting the switch from normal conidiation to microcycle conidiation. Previously, two genes, *mcb* and *mmc*, involved in the microcycle conidiation were identified in *N. crassa* and *M. anisopliae* (Maheshwari 1991; Liu et al. 2010). In this study, *mcb* and *mmc* were not different in the transcriptional levels between the $\Delta MaPpt1$ and WT strains, indicating that *MaPpt1* may play another role in microcycle conidiation. *FluG*, which is a negative regulator of fungal vegetative growth in *Aspergillus nidulans* (Rodriguez-Urra et al. 2012), was upregulated in $\Delta MaPpt1$, potentially promoting the microcycle conidiation. In *Trichoderma*, the nitrate assimilation regulatory protein nirA is required for phialide development (Schmoll et al. 2016), suggesting that downregulation of *nirA* might impair the normal aerial conidiation of $\Delta MaPpt1$. In $\Delta MaPpt1$, the LTE1 protein (MAC_03601) is upregulated, which is a regulator of mitotic exit and plays important roles in cell cycle control and polarized growth, as shown in *S. cerevisiae* (Seshan et al. 2002; Monje-Casas and Amon 2009; Geymonat et al. 2010). Cdc protein, directly or indirectly, controls LTE1 dephosphorylation and delocalization from the bud during exit from mitosis in *S. cerevisiae* (Seshan et al. 2002), suggesting that upregulation of Cdc48 broke spatial asymmetry of the LTE1 protein leading to cell cycle change in $\Delta MaPpt1$. Consequently, the change of cell cycle may lead to upregulation of the frequency clock protein gene (MAC_01916) in $\Delta MaPpt1$. From work in *N. crassa*, it is generally held that the normal conidiation cycle is partially the product of a

negative molecular feedback loop involving the rhythmic levels of frequency clock protein (Guo et al. 2010; Diernfellner and Schafmeier 2011). Mutation of the PKA-dependent phosphorylation sites on the phosphoprotein RCM-1 results in WC-independent transcription of frequency clock protein and impaired clock function in *Neurospora* (Liu et al. 2015). Frequency clock protein phosphorylations occur in the majority of the proteins involved and phosphorylation status influences their stability, activity, and subcellular localization (Diernfellner and Schafmeier 2011). DNA replication licensing factors, including *mcm2*, *mcm5*, and *mcm7*, were all upregulated in $\Delta MaPpt1$ -6 days. The minichromosome maintenance (MCM) complex is a putative DNA helicase complex that facilitates the initiation of DNA replication (Yoshida and Inoue 2003). MCM plays a critical role in DNA replication initiation and cell proliferation of eukaryotic cells (Wei et al. 2013). OxdC was present in the periplasm and remained firmly bound to cell-wall materials in *Collybia velutipes* (Azam et al. 2001). As demonstrated in *S. cerevisiae*, incorporation of cell wall protein in fungi can be completely determined by the timing of transcription during the cell cycle (Smits et al. 2006). Covalently linked cell wall protein gene (MAC_03347) was downregulated in the $\Delta MaPpt1$ strain, suggesting that MaPpt1 is also involved in fungal cell wall organization. In summary, these results indicated that the differential expression of genes involved in conidiation, cell cycle, cell proliferation, and cell wall organization potentially contributed to the enhanced formation of microcycle conidia in the $\Delta MaPpt1$ strain.

Besides increasing the ability of microcycle conidiation, deletion of *MaPpt1* also promoted the ability of the fungus to counteract UV irradiation which resulted in DNA damage. A number of repair or tolerant strategies were developed to counteract the DNA damage caused by UV in cells, such as photoreactivation, excision repair, and conidial pigmentation (Sinha and Häder 2002). Previous studies have reported that PP5 interacts with other proteins and influences cell cycle after DNA damage (Ali et al. 2004; Zhang et al. 2005; Yong et al. 2007). In mammalian systems and some lower eukaryotes including *Trypanosoma brucei* and *Toxocara canis*, loss or reduction of PP5/Ppt1 resulted in decreased ability to respond to DNA damage (Chaudhuri 2001; Ma et al. 2014). However, our data indicate that in *M. acridum*, Ppt1 acts as a negative regulator of DNA damage pathways, as the mutant strain was more resistant to UV exposure than the wild type and complementary strains. These results suggest that participation of PP5/Ppt1 in this pathway may conserve the outcome of its activity in DNA damage response has diverged. From DGE data, we found that 21 DNA damage repair-related genes were upregulated in $\Delta MaPpt1$. Of these genes, 4 genes are involved in base excision repair, including the genes for G-specific adenine glycosylase (Hašplová et al. 2012), DNA-3-methyladenine glycosylase (Troll et al. 2014), ADP-

ribosyltransferase (Eberle et al. 2015), and Rad7 (Venkannagari et al. 2016). Four genes are related to nucleotide excision repair, including the genes for ATP-dependent DNA ligase domain protein (Doherty and Wigley 1999), mating-type switching protein *swi10* (Rödel et al. 1999), and two DNA glycosylases (D'Errico et al. 2017; Lee and Wallace 2016). Two mismatch repair genes, encoding proliferating cell nuclear antigen (Emptage et al. 2008) and replication factor-A protein 1 (Emptage et al. 2008), are also included. In addition, the genes for DNA repair protein UVS6, which is known to be involved in UVB resistance and efficient DNA damage repair (Schroeder 1975), and DNA polymerase ϵ , which plays important roles in DNA damage tolerance repair (Fumasoni et al. 2015), were both upregulated in $\Delta MaPpt1$. Thus, the enhanced UV tolerances of $\Delta MaPpt1$ are likely due to upregulation of these DNA damage repair-related genes in *M. acridum*.

In summary, our results demonstrated that deletion of *MaPpt1* induced microcycle conidiation and conidia with higher UV tolerance, providing significant advantages to develop as control agents against insect pests. The deletion of *MaPpt1* increased conidial yield which is of benefit for industrial fermentation of biological control agents. This study provides new insight into dephosphorylation by the MaPpt1 regulator on microcycle conidiation and counteracting the DNA damage caused by UV. However, further work is needed to elucidate the molecular mechanisms of the process, with the genetic manipulation of MaPpt1 related to microcycle conidiation, more UV tolerance, being essential for the utilization of those biological control agents.

Funding This study was funded by Natural Science Foundation of China (No. 31272090), the Natural Science Foundation Project of Chongqing (CSTC 2018jcyjAX0554), and the Fundamental Research Funds for the Central Universities (106112017CDJQJ298831).

Compliance with ethical standards

Conflict of interest The authors declare that they have no conflict of interest.

Ethical approval This article does not contain any studies with human participants performed by any of the authors.

Publisher's Note Springer Nature remains neutral with regard to jurisdictional claims in published maps and institutional affiliations.

References

- Ali A, Zhang J, Bao S, Liu I, Otterness D, Dean NM, Abraham RT, Wang XF (2004) Requirement of protein phosphatase 5 in DNA-damage-induced ATM activation. *Genes Dev* 18:249–254
- Audic S, Claverie JM (1997) The significance of digital gene expression profiles. *Genome Res* 7:986–995

- Azam M, Kesarwani M, Natarajan K, Datta A (2001) A secretion signal is present in the *Collybia velutipes* oxalate decarboxylase gene. *Biochem Biophys Res Commun* 289:807–812
- Barford D (1996) Molecular mechanisms of the protein Ser/Thr phosphatases. *Trends Biochem Sci* 21:407–412
- Becker W, Kentrup H, Klumpp S, Schultz JE, Joost HG (1994) Molecular cloning of a protein serine/threonine phosphatase containing a putative regulatory tetratricopeptide repeat domain. *J Biol Chem* 269:22586–22592
- Bosch A, Yantorno O (1999) Microcycle conidiation in the entomopathogenic fungus *Beauveria bassiana* bals. (Vuill.). *Process Biochem* 34:707–716
- Chaudhuri M (2001) Cloning and characterization of a novel serine/threonine protein phosphatase type 5 from *Trypanosoma brucei*. *Gene* 266:1–13
- Chen MX, McPartlin AE, Brown L, Chen YH, Barker HM, Cohen P (1994) A novel human protein serine/threonine phosphatase, which possesses four tetratricopeptide repeat motifs and localizes to the nucleus. *EMBO J* 13:4278–4290
- Chinkers M (2001) Protein phosphatase 5 in signal transduction. *Trends Endocrinol Metab* 12:28–32
- D'Errico M, Parlanti E, Pascucci B, Fortini P, Baccarini S, Simonelli V, Dogliotti E (2017) Single nucleotide polymorphisms in DNA glycosylases: from function to disease. *Free Radic Biol Med* 107:278–291
- Das AK, Cohen PTW, Barford D (1998) The structure of the tetratricopeptide repeats of protein phosphatase 5: implications for TPR-mediated protein–protein interactions. *EMBO J* 17:1192–1199
- Dickman MB, Yarden O (1999) Serine/threonine protein kinases and phosphatases in filamentous fungi. *Fungal Genet Biol* 26:99–117
- Diernfellner ACR, Schafmeier T (2011) Phosphorylations: making the *Neurospora crassa* circadian clock tick. *FEBS Lett* 585:1461–1466
- Doherty AJ, Wigley DB (1999) Functional domains of an ATP-dependent DNA ligase. *J Mol Biol* 285:63–71
- dos Reis MC, Pelegrinelli Fungaro MH, Delgado Duarte RT, Furlaneto L, Furlaneto MC (2004) *Agrobacterium tumefaciens*-mediated genetic transformation of the entomopathogenic fungus *Beauveria bassiana*. *J Microbiol Methods* 58:97–202
- Du Y, Jin K, Xia Y (2018) Involvement of MaSom1, a downstream transcriptional factor of cAMP/PKA pathway, in conidial yield, stress tolerances, and virulence in *Metarhizium acridum*. *Appl Microbiol Biotechnol* 102:5611–5623
- Eberle RJ, Coronado MA, Caruso IP, Lopes DO, Miyoshi A, Azevedo V, Ami RK (2015) Chemical and thermal influence of the [4Fe–4S]²⁺ cluster of A/G-specific adenine glycosylase from *Corynebacterium pseudotuberculosis*. *Biochim Biophys Acta* 1850:393–400
- Emptage K, O'Neill R, Solovyova A, Connolly BA (2008) Interplay between DNA polymerase and proliferating cell nuclear antigen switches off base excision repair of uracil and hypoxanthine during replication in archaea. *J Mol Biol* 383:762–771
- Feng B, Zhao C, Tanaka S, Imanaka HK, Nakanishi K (2007) TPR domain of Ser/Thr phosphatase of *Aspergillus oryzae* shows no auto-inhibitory effect on the dephosphorylation activity. *Int J Biol Macromol* 41:281–285
- Fumasoni M, Zwicky K, Vanoli F, Lopes M, Branzei D (2015) Error-free DNA damage tolerance and sister chromatid proximity during DNA replication rely on the Pol α /Primase/Ctf4 Complex. *Mol Cell* 57:812–823
- Gao Q, Jin K, Ying S, Zhang Y, Xiao G, Shang Y, Duan Z, Hu X, Xie X, Zhou G, Peng G, Luo Z, Huang W, Wang B, Fang W, Wang S, Zhong Y, Ma L, St Leger RJ, Zhao G, Pei Y, Feng M, Xia Y, Wang C (2011) Genome sequencing and comparative transcriptomics of the model entomopathogenic fungi *Metarhizium anisopliae* and *M. acridum*. *PLoS Genet* 7:e1001264
- Geymonat M, Spanos A, Jensen S, Sedgwick SG (2010) Phosphorylation of Lte1 by Cdk prevents polarized growth during mitotic arrest in *S. cerevisiae*. *J Cell Biol* 191:1097–1112
- Guo JH, Cheng P, Liu Y (2010) Functional significance of FRH in regulating the phosphorylation and stability of *Neurospora* circadian clock protein FRQ. *J Biol Chem* 285:11508–11515
- Hašplová K, Hudecová A, Magdolénová Z, Bjørnas M, Gálová E, Miadoková E, Dušínská M (2012) DNA alkylation lesions and their repair in human cells: modification of the comet assay with 3-methyladenine DNA glycosylase (AlkD). *Toxicol Lett* 208:76–81
- Hu K, Li W, Gao J, Liu Q, Wang H, Wang Y, Sang J (2014) Role of Ppt1 in multiple stress responses in *Candida albicans*. *Chin Sci Bull* 59:4060–4068
- Jeong JY, Johns J, Sinclair C, Park JM, Rossie S (2003) Characterization of *Saccharomyces cerevisiae* protein Ser/Thr phosphatase T1 and comparison to its mammalian homolog PP5. *BMC Cell Biol* 4(3):3
- Kang Y, Cheong HM, Lee JH, Song PI, Lee KH, Kim SY, Jun JY, You HJ (2011) Protein phosphatase 5 is necessary for ATR-mediated DNA repair. *Biochem Biophys Res Commun* 404:476–481
- Kennelly PJ (2001) Protein phosphatases—a phylogenetic perspective. *Chem Rev* 101:2291–2312
- de la Fuente van Bentem S, Vossen JH, Vermeer JE, de Vroomen MJ, Gadella TW, Haring MA, Cornelissen BJ (2003) The subcellular localization of plant protein phosphatase 5 isoforms is determined by alternative splicing. *Plant Physiol* 133:702–712
- Lazo GR, Stein PA, Ludwig RA (1991) A DNA transformation competent *Arabidopsis* genomic library in *Agrobacterium*. *Biotechnology* 9:963–967
- Lee AJ, Wallace SS (2016) Visualizing the search for radiation-damaged DNA bases in real time. *Radiat Phys Chem Oxf Engl* 1993 128:126–133
- Li ZZ, Alves SB, Roberts DW, Fan MZ, Delalibera I, Tang J, Lopes RB, Faria M, Rangel DEN (2010) Biological control of insects in Brazil and China: history, current programs and reasons for their successes using entomopathogenic fungi. *Biocontrol Sci Tech* 20:117–136
- Liu J, Cao Y, Xia Y (2010) *Mmc*, a gene involved in microcycle conidiation of the entomopathogenic fungus *Metarhizium anisopliae*. *J Invertebr Pathol* 105:132–138
- Liu X, Li H, Liu Q, Niu Y, Hu Q, Deng H, Cha J, Wang Y, Liu Y, He Q (2015) Role for protein kinase A in the *Neurospora* circadian clock by regulating white collar-independent frequency transcription through phosphorylation of RCM-1. *Mol Cell Biol* 35:2088–2102
- Livak KJ, Schmittgen TD (2001) Analysis of relative gene expression data using real-time quantitative PCR and the 2^{- $\Delta\Delta$ CT} method. *Methods* 25:402–408
- Lomer CJ, Bateman RP, Johnson DL, Langewald J, Thomas M (2001) Biological control of locusts and grasshoppers. *Annu Rev Entomol* 46:667–702
- Luo S, He M, Cao Y, Xia Y (2013) The tetraspanin gene *MaPls1* contributes to virulence by affecting germination, appressorial function and enzymes for cuticle degradation in the entomopathogenic fungus *Metarhizium acridum*. *Environ Microbiol* 15:2966–2979
- Ma GX, Rong QZ, Shi JH, Han CH, Tao Z, Xia QY (2014) Molecular characterization and functional analysis of serine/threonine protein phosphatase of *Toxocara canis*. *Exp Parasitol* 141:55–61
- Maheshwari R (1991) Microcycle conidiation and its genetic basis in *Neurospora crassa*. *J Gen Microbiol* 137:2103–2115
- Ming Y, Wei Q, Jin K, Xia Y (2014) MaSnf1, a sucrose non-fermenting protein kinase gene, is involved in carbon source utilization, stress tolerance, and virulence in *Metarhizium acridum*. *Appl Microbiol Biotechnol* 98:10153–10164
- Monje-Casas F, Amon A (2009) Cell polarity determinants establish asymmetry in MEN signaling. *Dev Cell* 16:132–145
- Ortiz-Urquiza A, Keyhani NO (2013) Action on the surface: entomopathogenic fungi versus the insect cuticle. *Insects* 4:357–374

- Ortiz-Urquiza A, Luo Z, Keyhani NO (2015) Improving mycoinsecticides for insect biological control. *Appl Microbiol Biotechnol* 99:1057–1068
- Rangel DEN, Braga GUL, Fernandes ÉKK, Keyser CA, Hallsworth JE, Roberts DW (2015) Stress tolerance and virulence of insect-pathogenic fungi are determined by environmental conditions during conidial formation. *Curr Genet* 61:383–404
- Rödel C, Jupitz T, Schmidt H (1999) Complementation of the DNA repair-deficient *swi10* mutant of fission yeast by the human *ERCC1* gene. *Nucleic Acids Res* 25:2823–2827
- Rodriguez-Urra AB, Jimenez C, Nieto MI, Rodriguez J, Hayashi H, Ugalde U (2012) Signaling the induction of sporulation involves the interaction of two secondary metabolites in *Aspergillus nidulans*. *ACS Chem Biol* 7:599–606
- Schmoll M, Dattenböck C, Carrerasvillaseñor N, Mendozamendoza A, Tisch D, Alemán MI, Baker SE, Brown C, Cervantes-Badillo MG, Cetz-Chel J, Cristobal-Mondragon GR, Delaye L, Esquivel-Naranjo EU, Frischmann A, Gallardo-Negrete Jde J, García-Esquivel M, Gomez-Rodriguez EY, Greenwood DR, Hernández-Oñate M, Kruszewska JS, Lawry R, Mora-Montes HM, Muñoz-Centeno T, Nieto-Jacobo MF, Nogueira Lopez G, Olmedo-Monfil V, Osorio-Concepcion M, Piłsyk S, Pomraning KR, Rodriguez-Iglesias A, Rosales-Saavedra MT, Sánchez-Arreguín JA, Seidl-Seiboth V, Stewart A, Uresti-Rivera EE, Wang CL, Wang TF, Zeilinger S, Casas-Flores S, Herrera-Estrella A (2016) The genomes of three uneven siblings: footprints of the lifestyles of three *Trichoderma* species. *Microbiol Mol Biol Rev* 80:205–327
- Schroeder A (1975) Genetic control of radiation sensitivity and DNA repair in *Neurospora*. *Basic Life Sci* 5B:567–576
- Schwede T, Kopp J, Guex N, Peitsch M (2003) SWISS-MODEL: an automated protein homology-modeling server. *Nucleic Acids Res* 31:3381–3385
- Seshan A, Bardin AJ, Amon A (2002) Control of Lte1 localization by cell polarity determinants and Cdc14. *Curr Biol* 12:2098–2110
- Shi Y (2009) Serine/threonine phosphatases: mechanism through structure. *Cell* 139:468–484
- Sinha RPS, Häder DP (2002) UV-induced DNA damage and repair: a review. *Photochem Photobiol Sci* 1:225–236
- Smits GJ, Schenkman LR, Brul S, Pringle JR, Klis FM (2006) Role of cell cycle-regulated expression in the localized incorporation of cell wall proteins in yeast. *Mol Biol Cell* 17:3267–3280
- Troll CJ, Adhikary S, Cuff M, Mitra I, Eichman BF, Camps M (2014) Interplay between base excision repair activity and toxicity of 3-methyladenine DNA glycosylases in an *E. coli* complementation system. *Mutat Res* 763–764: 64–73, 763–764
- Venkannagari H, Verheugd P, Koivunen J, Haikarainen T, Obaji E, Ashok Y, Narwal M, Pihlajaniemi T, Lüscher B, Lehtiö L (2016) Small-molecule chemical probe rescues cells from mono-ADP-ribosyltransferase ARTD10/PARP10-induced apoptosis and sensitizes cancer cells to DNA damage. *Cell Chem Biol* 23:1251–1260
- Wandinger SK, Suhre MH, Wegele H, Buchner J (2006) The phosphatase Ppt1 is a dedicated regulator of the molecular chaperone Hsp90. *EMBO J* 25:367–376
- Wei Q, Li JH, Liu T, Tong XM, Ye X (2013) Phosphorylation of minichromosome maintenance protein 7 (MCM7) by cyclin/cyclin-dependent kinase affects its function in cell cycle regulation. *J Biol Chem* 288:19715–19725
- Yong W, Bao S, Chen H, Li D, Sánchez ER, Shou W (2007) Mice lacking protein phosphatase 5 are defective in ataxia telangiectasia mutated (ATM)-mediated cell cycle arrest. *J Biol Chem* 282:14690–14694
- Yoshida K, Inoue I (2003) Conditional expression of MCM7 increases tumor growth without altering DNA replication activity. *FEBS Lett* 553:213–217
- Zhang LB, Feng MG (2018) Antioxidant enzymes and their contributions to biological control potential of fungal insect pathogens. *Appl Microbiol Biotechnol* 102:4995–5004
- Zhang J, Bao S, Furumai R, Kucera KS, Ali A, Dean NM, Wang XF (2005) Protein phosphatase 5 is required for ATR-mediated checkpoint activation. *Mol Cell Biol* 25:9910–9919
- Zhang S, Peng G, Xia Y (2010) Microcycle conidiation and the conidial properties in the entomopathogenic fungus *Metarhizium acridum* on agar medium. *Biocontrol Sci Tech* 20:809–819